Journal of Statistical Physics, Vol. 110, Nos. 3–6, March 2003 (© 2003)

Debye–Hückel Theory for Charged Aligned Needles and for Polyelectrolyte Solutions

Johan Høye,[1] Fernando O. Raineri,[2] George Stell,[2] and Jennifer Routh[2]

Received April 25, 2002; accepted July 18, 2002

We consider a simple extension of the familiar Debye–Hückel theory of electrolyte solutions (in which the ions are represented by spheres with embedded point charges) to study the thermodynamic properties and the phase diagram of ionic solutions in which the ions of at least one of the species are deformed into parallel and rigid needle-like ellipsoidal objects that have a continuous line of charge distribution along their axis of revolution. We examine two specific cases: (a) solutions comprising both cationic and anionic needles that are identical in every respect except for the charge sign, and (b) solutions in which only one ionic species is made up of parallel rigid needles while the other species is made up of point ions. The first system is the analog, for ionic needles, of the familiar restricted primitive model of electrolytes, while the second one is a very simple model for a polyelectrolyte solution. For both systems we investigate how the phase diagram is affected by the extent of deformation of the ions, as measured by the spatial spread of their charge distribution.

KEY WORDS: Charged-aligned needles; polyelectrolyte solutions; charge distribution; Debye–Hückel; phase separation; coexistence line; critical parameters.

1. INTRODUCTION

The last decade has witnessed extraordinary interest in understanding and characterizing the phenomenon of phase separation in electrolyte solutions, in which two liquid phases of different electrolyte concentrations coexist in equilibrium.[1,2] The related question concerning the critical exponents of the associated critical point has also received extensive scrutiny.[1,2]

By far the bulk of this theoretical activity has focused on the restricted primitive model (RPM) of an electrolyte solution. This is a symmetric

[1] Institutt for Fysikk, NTNU, N 7491 Trondheim, Norway; e-mail: hoye@phys.ntnu.no
[2] Department of Chemistry, State University of New York at Stony Brook, Stony Brook, New York 11794-3400, USA; e-mail: raineri@mail.chem.sunysb.edu

0022-4715/03/0300-0835/0 © 2003 Plenum Publishing Corporation

model formulated at the McMillan–Mayer level,[3,4] in which the solvent-averaged interactions between the ions are represented by the interactions between hard spheres with embedded point charges. Except for the sign of their charges, cations and anions in the RPM are identical. The instability with respect to phase separation has also been investigated, to a lesser degree, for size- and/or charge-asymmetric primitive models of electrolyte solutions.[2,5–8] So-called civilized models, which dispense with the hard-sphere representation of the short-range interactions, have also been considered.[9]

The techniques employed in these studies include computer simulations, Ornstein–Zernike integral equation studies implemented with a variety of closure relations, as well as simpler mean-field theories constructed by piecing together various contributions to the Helmholtz free energy. In many of the analytical approaches allowance is made for chemical association of anions and cations to form ion pairs or larger clusters.

While these theories can account for the fact that in certain range of temperature and concentration an ionic solution becomes unstable against phase separation into two liquid phases of different concentration, they have not been entirely succesful in accurately predicting the location of the critical point. However, the theoretical efforts and experiment agree in that the coexistence line is quite asymmetric; the positive slope of the low concentration branch being considerably steeper than the negative slope of the high concentration branch. In fact the asymmetry of the coexistence line is strikingly reminiscent of the coexistence line in polymer systems.

In the polymer case, the degree of asymmetry of the coexistence line is a sensitive function of the mean number of monomeric units N of the chain polymers. In mean-field theories, such as that of Flory and Huggins, as N goes from $N=1$ to $N=\infty$, the coexistence curve goes from a simple Bragg–Williams or van der Waals form to one in which the critical number density ρ_{crit} goes to zero.[10] This prompted Michael Fisher to ask in his Onsager Symposium lecture[1] whether there is any analogous control parameter for the RPM representation of an electrolyte solution.

One answer was given by Stell in his Onsager Symposium contribution[2] on the basis of work done by Høye and Stell, who noted that $2/(d-2)$, where d is the spatial dimensionality, can play the role of N for the RPM. Here the d-dimensional RPM particles are defined by hard d-dimensional hyperspheres plus Coulomb interactions that satisfy Laplace's equation in d dimensions. A simple mean-field theory that illustrates the analogy with the Flory–Huggins polymer result is given by an equation of state that has the hard-hypersphere contribution appropriate to low density in any dimension, $\beta P_r = \rho/(1-B\rho)$, (where $\beta = (k_{\text{B}}T)^{-1}$ is the inverse of the temperature expressed in energy units, P is the pressure, and B is the

second virial coefficient) plus the dominant Coulombic contribution, which in $3d$ is given by the well known expression $(\beta P_q)_3 = -\varkappa^3/24\pi$ (where $\varkappa$ is the inverse Debye shielding length). This Coulomb-related term can be alternatively represented as $(\beta P_q)_3 = -A_3(\beta\rho)^{3/2}$, with $A_3 = \pi^{1/2}q^3/3\epsilon^{3/2}$ (where q is the magnitude of the ionic charge and ϵ is the dielectric constant of the medium). In d dimensions, this becomes $(\beta P_q)_d = -A_d(\beta\rho)^{d/2}$, with $A_d = \text{constant} \times q^d$, to yield the equation of state

$$(\beta P)_d = (\beta P_r)_d + (\beta P_q)_d = \frac{\rho}{1-B\rho} - A_d(\beta\rho)^{d/2}.$$

For $d = 4$ this is exactly of van der Waals form. For any $2 \leqslant d \leqslant 4$, $B\rho_{\text{crit}} = (d-2)/(d+2)$, so that in the $d \to 2$ limit $\rho_{\text{crit}} \to 0$.

Subsequently, Fisher and coauthors used more refined Debye–Hückel-based mean-field theories for the RPM to study the $d \to 2$ limit, and showed that one obtains many of the features of the Kosterlitz–Thouless transition that is expected in that limit from their approximation.[11]

The parameter $2/(2-d)$ is not experimentally accessible, leading Stell and Høye to inquire whether one could find a physically realizable sequence (keeping $d = 3$) that is like changing d from 4 to 2 (or at least 3 to 2, since one is starting at 3). In a preliminary investigation they concluded in the affirmative, and that such a sequence can be provided by distorting the charged spheres of diameter σ into parallel charged ellipsoids of major axes a, b, and c, with $\sigma^3 = abc = a^2c$, with a line of charge running along the axis of revolution of each ellipsoid. As we approach the infinitely long-needle limit, $c \to \infty$, we again expect the same change in coexisting-curve symmetry. This paper describes the details of this limiting process as well as a closely related one in which only the spheres of one charge sign are elongated, with the spheres of the opposite charge remaining charged spheres of arbitrarily small diameter, which we treat simply as point ions.

The system of charged needles and oppositely charged counterions shares many of the features of models that are used to study polyelectrolyte solutions, but there are certain key differences between our treatment here and current treatments[12] of such polyelectrolyte models. On the one hand, we assume that our needles are constrained to remain parallel or nematically ordered, so that we are unable to address the key issue of the isotropic-nematic transition in a polyelectrolyte solution. On the other hand, we begin with a model in which the interaction between charge elements is given by a Coulombic potential, rather than a preaveraged potential of mean force of Debye–Hückel (i.e., Yukawa) form. In this regard, our treatment is a highly sophisticated one, since we explicitly do the statistical-mechanical summation that introduces the Debye shielding between charge elements.

In future work we hope to refine our theory by introducing Bjerrum type association and charge dipole interactions. We also intend to extend the model by allowing a distribution of orientations among the needles.

To calculate the thermodynamic properties of these model systems we focus on the McMillan–Mayer level thermodynamic potential $I \equiv -\beta A/V$, defined in terms of the Helmholtz free energy A of the ionic system and the volume V of the solution.[3,4] We approximate I by the sum

$$I = I_r + I_q, \tag{1.1}$$

where the reference part $I_r = -\beta A_r/V$ incorporates both the ideal (or noninteracting) contribution as well as the contribution from the non-electrostatic short-range interactions between the ions to the excess Helmholtz free energy. Correspondingly, $I_q = -\beta A_q/V$ originates from the long-range electrostatic interactions between the ions. In our approach I_r and I_q are calculated independently of each other. In particular we estimate I_q by means of a simple extension of the familiar Debye–Hückel theory of electrolyte solutions to the case in which the charge distribution of the ions has non-zero spatial extent.

The outline of the paper is as follows. We begin in Section 2 with a brief summary of the Debye–Hückel result for the electrostatic contribution I_q in the case of an electrolyte solution comprising point ions. In Section 3 we consider solutions of charged needles, where we develop, in turn, (i) the generalization of the point-ion Debye–Hückel result for I_q obtained in Section 2 to charged aligned needles, (ii) the derivation of an expression for the osmotic pressure of the solution of needle-like ions as a function of the ionic number density ρ and the temperature (equation of state in the McMillan–Mayer system of variables), and finally (iii) the derivation of approximate expressions, valid for sufficiently long needles, for the dependence of the critical temperature T_{crit} and critical density ρ_{crit} with the inverse range parameter γ that characterizes the spatial spread of the charge distribution of a needle-like ion. In Section 4 we report similar results for a very simple representation of a polyelectrolyte solution, in which the polyelectrolyte ions are represented by charged aligned needles and the counterions are represented by point charges. In Section 5 we present the results of numerical calculations of the coexistence line for the liquid–liquid phase equilibrium for both sytems. We also report, again for both electrolyte systems, the parametric dependence of the critical temperature and critical density with the inverse charge range parameter γ, spanning the range from point ions to very long needles. In Section 6 we present a brief summary of the results reported in Sections 3–5. In Appendix A we briefly examine the expressions for the needle–needle correlation functions calculated at the Debye–Hückel level.

2. DEBYE–HÜCKEL THEORY FOR POINT CHARGES

In Gaussian units the interaction between two point charges in a continuum medium of dielectric constant ϵ is

$$\phi_{ij}(r) = q_i q_j / \epsilon r, \tag{2.1}$$

where q_i and q_j are the charges of particles i and j, while r is their separation. The Fourier transform $\tilde{\phi}_{ij}(k)$ in three-dimensional space of $\phi_{ij}(r)$ is

$$\tilde{\phi}_{ij}(k) = 4\pi q_i q_j / \epsilon k^2. \tag{2.2}$$

The contribution to the free energy from this interaction is, in the Debye–Hückel approximation, obtained by summation of the ring graphs where the bonds are potential energy bonds, and the vertices are simple ρ-vertices. In evaluating these graphs one has convolutions in Fourier space, and summation of all of them yields the electrostatic contribution I_q to the thermodynamic potential I [cf. Eq. (1.1)]:

$$I_q = -\frac{1}{2}\int \frac{d^3\mathbf{k}}{(2\pi)^3}\left[\ln\left(1+\frac{\varkappa^2}{k^2}\right)-\frac{\varkappa^2}{k^2}\right]. \tag{2.3}$$

The temperature and density of the solution are collected in the Debye inverse shielding length $\varkappa$, as shown in the equation

$$\varkappa^2 = \frac{4\pi\beta}{\epsilon}\sum_i q_i^2 \rho_i. \tag{2.4}$$

Here ρ_i is the number density of the ionic species i in the solution. By evaluation of Eq. (2.3) one obtains the well known Debye–Hückel result

$$I_q = \frac{\varkappa^3}{12\pi} \tag{2.5}$$

for the electrostatic contribution to the thermodynamic potential I.

In this simple derivation the effect of the ionic hard cores is neglected. This effect is taken into account when applying the MSA (mean spherical approximation). In the MSA the graph sum (2.3) still applies, but the interaction inside the hard core radius is modified such that when evaluating the corresponding pair-correlation function the hard-core condition is fulfilled.

3. CHARGED NEEDLES

We consider a solution of a binary electrolyte comprising $N_+ = N/2$ nonspherical cations of charge q and $N_- = N/2$ nonspherical anions of charge $-q$ dissolved in a solvent (modeled as a continuum dielectric medium) of dielectric constant ϵ. The cations and anions are identical in every respect, except for the sign of their charges. Furthermore, as explained in the introduction, the charge q in an ion is not concentrated in a single point within the ion.

The square of Debye inverse shielding length for this model is $\varkappa^2 = 4\pi\beta q^2\rho/\epsilon$, where $\rho \equiv \rho_+ + \rho_-$ is the total number density of ions in the solution.

3.1. The Electrostatic Contribution I_q

We will not attempt to use the mean spherical approximation to calculate the thermodynamic potential I, as the core condition for nonspherical ions will be much more complex to handle compared to the case of spherical ions. Instead, we consider separate and independent estimates for the reference I_r and electrostatic I_q parts to I.

For the electrostatic part we adopt a straightforward generalization of the calculation of I_q for spherical ions summarized in Section 2. We represent the charge density of an ion by $\pm q\Lambda(\mathbf{r})$, where the plus and minus sign apply, respectively, to the cationic and anionic species. Notice that the coordinate $\mathbf{r}$ refers to the location of a point inside the ion measured relative to the center of the ion; and of course the density function $\Lambda(\mathbf{r})$ is normalized in such a way that $\int d\mathbf{r}\, \Lambda(\mathbf{r}) = 1$.

The electrostatic contribution to the potential energy of interaction between any two ions i and j, with centers located at $\mathbf{r}_i$ and $\mathbf{r}_j$, is given by the convolution integral

$$\psi_{ij}(\mathbf{r}_{ij}) = \int d^3\mathbf{x} \int d^3\mathbf{x}'\, \Lambda(\mathbf{x}-\mathbf{r}_i)\, \phi_{ij}(|\mathbf{x}-\mathbf{x}'|)\, \Lambda(\mathbf{x}'-\mathbf{r}_j), \tag{3.1}$$

where $\mathbf{r}_{ij} \equiv \mathbf{r}_i - \mathbf{r}_j$ and $\phi_{ij}(|\mathbf{x}-\mathbf{x}'|) = q_i q_j/\epsilon\,|\mathbf{x}-\mathbf{x}'|$ is the Coulomb interaction between two point charges q_i and q_j located at points $\mathbf{x}$ and $\mathbf{x}'$ [compare with Eq. (2.1)]. Taking the Fourier transform of both sides of Eq. (3.1) we obtain the simpler form

$$\tilde{\psi}_{ij}(\mathbf{k}) = \tilde{\Lambda}(-\mathbf{k})\, \tilde{\phi}_{ij}(k)\, \tilde{\Lambda}(\mathbf{k}), \tag{3.2}$$

where $\tilde{\phi}_{ij}(k)$ is given in Eq. (2.2) and

$$\tilde{\Lambda}(\mathbf{k}) = \int d^3\mathbf{r}\, e^{i\mathbf{k}\cdot\mathbf{r}}\, \Lambda(\mathbf{r}). \tag{3.3}$$

For electrolyte solution models in which the ions are deformed into needles aligned along the z-axis the charge density function takes the form $\Lambda(\mathbf{r}) = \delta(x)\,\delta(y)\,\lambda(z)$, for which Eq. (3.3) simplifies to

$$\tilde{\Lambda}(\mathbf{k}) = \tilde{\lambda}(k_z) = \int_{-\infty}^{\infty} dz\, e^{ik_z z}\, \lambda(z), \tag{3.4}$$

where k_z is the projection of the wavevector $\mathbf{k}$ along the z-axis. Thence, for needle-like ions, Eq. (3.2) reduces to

$$\tilde{\psi}_{ij}(\mathbf{k}) = \tilde{\phi}_{ij}(k)\, F(k_z), \tag{3.5}$$

where the charge form factor

$$F(k_z) = \tilde{\lambda}(-k_z)\,\tilde{\lambda}(k_z) = |\tilde{\lambda}(k_z)|^2, \tag{3.6}$$

depends only on k_z in the case that the ions are parallel needles.

We now consider the calculation of I_q by a procedure similar to the diagramatic method outlined in Section 2 for electrolyte solutions comprising spherical ions. If the needles, as is the case we want to focus upon here, are aligned along the z-axis, the previous ρ-vertex becomes now a function of k_z. This k_z-dependence will then enter through the function

$$\varkappa^2(k_z) = \varkappa^2 F(k_z) \tag{3.7}$$

where $\varkappa^2$ and $F(k_z)$ were introduced, respectively, in Eqs. (2.4) and (3.6). Summation of the modified graphs leads to a result for I_q for a solution of charged needles that is the generalization of Eq. (2.3) for spherical ions:

$$I_q = \int_{-\infty}^{\infty} \frac{dk_z}{2\pi}\, I_q(k_z), \tag{3.8}$$

where

$$I_q(k_z) = \int \frac{d^2\mathbf{k}_\perp}{(2\pi)^2} \left\{ -\frac{1}{2}\left[\ln\left(1 + \frac{\varkappa^2(k_z)}{k_\perp^2 + k_z^2}\right) - \frac{\varkappa^2(k_z)}{k_\perp^2 + k_z^2} \right] \right\}. \tag{3.9}$$

Clearly the argument of the double integral in Eq. (3.9) is basically the same as the argument in the integral of Eq. (2.3); the only difference is the

replacement of $\varkappa^2$ in Eq. (2.3) by the function $\varkappa^2(k_z)$ [cf. Eq. (3.7)], which is a consequence of the non-zero spatial extent of the charge distribution in the case of needles. This difference forces us to carry out the calculation of I_q by performing the integration over the wavevector in two steps: first perform the integral with respect to $\mathbf{k}_\perp = (k_x, k_y)$ to obtain $I_q(k_z)$, Eq. (3.9), followed by integration with respect to k_z to obtain I_q, Eq. (3.8).

The evaluation of $I_q(k_z)$ from Eq. (3.9) is straightforward; we find

$$I_q(k_z) = -\frac{1}{8\pi}\left\{\varkappa^2(k_z) - [k_z^2 + \varkappa^2(k_z)] \ln\left(1 + \frac{\varkappa^2(k_z)}{k_z^2}\right)\right\}. \tag{3.10}$$

It is interesting to examine this expression for $I_q(k_z)$ of a solution of needle-like ions in the limit when $k_z = k_0$ very small (but not zero), such that both $k_0 \ll \varkappa$ and $F(k_0) \simeq 1$ are satisfied. This last relation follows from Eq. (3.4) and the normalization condition for the charge density function $\Lambda(\mathbf{r})$. In this limit $I_q(k_z)$ given in Eq. (3.10) becomes identical to I_q for a 2-dimensional ($2d$) Coulomb gas of point ions:

$$(I_q)_{2d} = -\frac{1}{8\pi}\varkappa_{2d}^2\left[1 - \ln\frac{\varkappa_{2d}^2}{k_0^2}\right] \tag{3.11}$$

where $\varkappa_{2d}^2 = 2\pi\beta q^2\rho$, which should be contrasted with the expression for $\varkappa^2$ for the solution of charged needles.

In order to calculate I_q with Eq. (3.8) we must first specify the charge density function $\lambda(z)$ for a needle-like ion. Ideally, we would choose $\lambda(z) = 1/\ell$ for z such that $|z| \leqslant \ell/2$ and $\lambda(z) = 0$ for $|z| \geqslant \ell/2$, where ℓ is the distance between the foci of the ellipsoid through its axis of revolution (recall that the ellipsoid results from the deformation of a spherical ion along the z-axis). This particular form of $\lambda(z)$ corresponds to a foci-to-foci line of uniform charge density along the primary axis of the ellipsoid. The corresponding one dimensional Fourier transform $\tilde{\lambda}(k_z)$ [cf. Eq. (3.4)] is $\tilde{\lambda}(k_z) = j_0(k_z\ell/2)$, where $j_0(x) = \sin(x)/x$ is the spherical Bessel function of order zero. It then follows from Eqs. (3.6) and (3.7) that $\varkappa^2(k_z)$ in Eq. (3.9) is given by $\varkappa^2(k_z) = \varkappa^2\, j_0(k_z\ell/2)^2$.

While it should be possible to perform the integral in Eq. (3.8) numerically with this form of $\varkappa^2(k_z)$, in this work we adopt a more convenient model for $\lambda(z)$ that allows us to perform the integrals analytically. Our simpler choice for $\lambda(k_z)$ is

$$\tilde{\lambda}(k_z) = \begin{cases} 1 & \text{for} \quad |k_z| < \gamma \\ 0 & \text{for} \quad |k_z| > \gamma, \end{cases} \tag{3.12}$$

where the parameter γ represents the inverse range of the charge distribution of a needle. By performing the inverse Fourier transform of $\tilde{\lambda}(k_z)$ we find that the charge of a needle is distributed according to the function

$$\lambda(z) = \int_{-\infty}^{\infty} \frac{dk_z}{2\pi} e^{ik_z z} \tilde{\lambda}(k_z) = \int_{-\gamma}^{\gamma} \frac{dk_z}{2\pi} e^{ik_z z} = \frac{\gamma}{\pi} \frac{\sin(\gamma z)}{\gamma z}. \tag{3.13}$$

It is important to point out the behaviour of this choice for $\lambda(z)$ with the inverse length parameter γ. From $\lim_{\gamma \to \infty} [\sin(\gamma z)/\pi z] = \delta(z)$ we conclude that the model $\tilde{\lambda}(k_z)$ given by Eq. (3.12) recovers, when $\gamma \to \infty$, the charge density $\Lambda(r) = \delta(\mathbf{r})$ of a point ion. Conversely, invoking the relation $\lim_{\gamma \to 0} [\sin(\gamma z)/(\gamma z)] = 1$, we observe that for $\gamma \simeq 0$ and $z \ll \gamma^{-1}$ the charge density $\tilde{\lambda}(k_z)$ given by Eq. (3.12) implies $\lambda(z) = \gamma/\pi$ independent of z; this corresponds to an infinitely long needle of uniform charge.

It then seems reasonable to consider Eqs. (3.12) and (3.13) as approximations to the more realistic expressions for $\tilde{\lambda}(k_z)$ and $\lambda(z)$ discussed in the previous paragraph. From this viewpoint we may interpret $2\pi/\gamma$ as a measure of the length of the needles.

With Eq. (3.12) for $\tilde{\lambda}(k_z)$, the wavevector-dependent function $\varkappa^2(k_z)$ becomes [cf. Eq. (3.7)]

$$\varkappa^2(k_z) = \begin{cases} \varkappa^2 & \text{for } |k_z| < \gamma \\ 0 & \text{for } |k_z| > \gamma. \end{cases} \tag{3.14}$$

This simple expression allows us to calculate the integral in Eq. (3.8) to obtain I_q. We find

$$I_q = \int_{-\gamma}^{\gamma} \frac{dk_z}{2\pi} I_q(k_z) = \frac{\varkappa^3}{24\pi^2} \left[-\frac{1}{x} + \left(\frac{3}{x} + \frac{1}{x^3} \right) \ln(1+x^2) + 4 \operatorname{Arctan}\left(\frac{1}{x} \right) \right], \tag{3.15}$$

where, for convenience, we have introduced the auxilliary variable $x \equiv \varkappa/\gamma$.

As expected from the discussion in the paragraph following Eq. (3.13), I_q given by Eq. (3.15) recovers Eq. (2.5) in the point-ion limit $\gamma \to \infty$. In the opposite $\gamma \to 0$ limit (infinitely long needles), I_q adquires the form of the 2-dimensional result $(I_q)_{2d}$, Eq. (3.11), but with $\varkappa_{2d}^2$ replaced by $\varkappa^2\gamma/\pi$, which represents a renormalization of the charge consistent with the 2-dimensional interaction along the needles.

3.2. Equation of State for Solutions of Charge Needles

We can calculate the osmotic pressure P of the solution from the thermodynamic potential I using the relation

$$\beta P = I - \rho \left(\frac{\partial I}{\partial \rho} \right)_T, \tag{3.16}$$

where ρ is the total ionic number density. Assuming the partition of I discussed in Section 1, Eq. (1.1), we may decompose the osmotic pressure into reference P_r and electrostatic P_q contributions

$$\beta P = \beta P_r + \beta P_q. \tag{3.17}$$

The electrostatic contribution P_q may be calculated by performing the calculation implied by the right hand hand of Eq. (3.16) on I_q given by Eq. (3.15). Alternatively, we may first calculate the intermediate quantity $P_q(k_z)$ defined by (exploiting the fact that $\varkappa^2$ is proportional to the total ionic density ρ)

$$\beta P_q(k_z) = I_q(k_z) - \varkappa^2 \left(\frac{\partial I_q(k_z)}{\partial \varkappa^2} \right)_T, \tag{3.18}$$

and, afterwards, integrate the result with respect to k_z in the way instructed by Eq. (3.8)

$$\beta P_q = \int_{-\infty}^{\infty} \frac{dk_z}{2\pi} \beta P_q(k_z). \tag{3.19}$$

Both procedures give, of course, the same result. The second route is somewhat more interesting, as the result for $P_q(k_z)$ that we derive from $I_q(k_z)$ given by Eq. (3.10) is valid for any form of the charge density function $\lambda(z)$. We obtain

$$\beta P_q(k_z) = -\frac{1}{8\pi} \left\{ \varkappa^2(k_z) - k_z^2 \ln \left(1 + \frac{\varkappa^2(k_z)}{k_z^2} \right) \right\}. \tag{3.20}$$

It is interesting to examine this result in the limit $k_z \to 0$, at which $F(k_z = 0) = 1$. In this limit Eq. (3.20) reduces to $\beta P_q(k_z = 0) = -\varkappa^2/8\pi$, which is directly comparable to the equation of state for the 2-dimensional Coulomb gas $\beta(P_q)_{2d} = -\varkappa_{2d}^2/8\pi$. This equivalence is, of course, not unexpected, in view that a similar equivalence holds at the level of the thermodynamic potential $I_q(k_z)$ [cf. Eqs. (3.10) and (3.11)].

The electrostatic contribution P_q to the pressure is obtained from the integration of $P_q(k_z)$ with respect to the wavevector as indicated in Eq. (3.19). For this step we require a specific model for the function $\varkappa^2(k_z)$. With Eqs. (3.14) and (3.20) we calculate

$$\beta P_q = \int_{-\gamma}^{\gamma} \frac{dk_z}{2\pi} \beta P_q(k_z) = -\frac{\varkappa^3}{24\pi^2} f(x), \tag{3.21}$$

where we have introduced the auxilliary function

$$f(x) = 2\,\mathrm{Arctan}(1/x) + (1/x) - (1/x^3)\ln(1+x^2), \tag{3.22}$$

with the variable x defined again as $x = \varkappa/\gamma$.

To complete the calculation of the osmotic pressure P we need to specify the reference part P_r. In this work we describe this contribution with the Percus–Yevick equation for hard spheres[4, 13]

$$\beta P_r = \rho \frac{1+\eta+\eta^2}{(1-\eta)^3}, \tag{3.23}$$

where $\eta = (\pi/6)\,\rho\sigma^3$ is the packing fraction and ρ is the total ionic number density of the solution. Equation (3.23) may also be used to calculate the reference contribution to the pressure for lined up ellipsoids, as they can be obtained from ions of diameter σ by simply stretching them along their z-axis.[14]

The total osmotic pressure of the solution (ideal plus excess parts) is then obtain by the sum of P_r, Eq. (3.23), and P_q, Eq. (3.21).

3.3. Critical Parameters for Solutions of Long Charged Aligned Needles

When one examines the dependence of the osmotic pressure P with ρ and T it becomes obvious that there is a region of the T-ρ plane for which

$$\left(\frac{\partial(\beta P)}{\partial \rho}\right)_T = \frac{\rho}{2}\left(\frac{\partial(\beta\mu)}{\partial\rho}\right)_T < 0, \tag{3.24}$$

where μ is the chemical potential of the electrolyte (i.e., μ is the chemical potential of the neutral pairs of particles with density $\rho/2$).[9] The realization of inequality (3.24) is the signature that the solution of charged aligned needles becomes unstable against phase separation into two liquid phases of different concentration.[9] In Section 5 we examine in some detail the

coexistence line for this liquid–liquid phase equilibrium; presently we derive simple analytical expressions for the dependence of the critical parameters T_{crit} and ρ_{crit} with inverse charge range parameter γ for solutions comprising long needles (γ small).

To obtain the location of the critical point of the solution we have to find where the first and second derivatives of P vanish:

$$\text{(a)} \quad \left(\frac{\partial(\beta P)}{\partial \rho}\right)_T = 0; \qquad \text{(b)} \quad \left(\frac{\partial^2(\beta P)}{\partial \rho^2}\right)_T = 0, \qquad \text{at critical.} \tag{3.25}$$

To implement these conditions we shall assume that the critical density ρ_{crit} is very small, so that we may approximate Eq. (3.23) for P_r by the first few terms in its power series expansion with respect to ρ:

$$\beta P_r \simeq \rho(1+4\eta+\cdots), \tag{3.26}$$

From Eqs. (3.17), (3.21), and (3.26) we calculate

$$\left(\frac{\partial(\beta P)}{\partial \rho}\right)_T = 1+8\eta-\frac{\varkappa^3}{8\pi^2\rho}g(x), \tag{3.27}$$

where we have introduced the auxilliary function

$$g(x)=\frac{1}{6}[3f(x)+x\,f'(x)] = \text{Arctan}\left(\frac{1}{x}\right), \tag{3.28}$$

and where the prime in $f'(x)$ indicates the derivative of the function with respect to the variable x. The second equality follows straightforwardly from the definition of $f(x)$ [cf. Eq. (3.22)].

From Eq. (3.27) we can calculate the second derivative of βP with respect to the total ionic density. We find:

$$\left(\frac{\partial^2(\beta P)}{\partial \rho^2}\right)_T = 8\frac{\eta}{\rho}-\frac{\varkappa^3}{16\pi^2\rho^2}[g(x)+xg'(x)]. \tag{3.29}$$

Assuming that at critical η is small the term 8η can be neglected in Eq. (3.27). Then at criticality, the right hand side of Eqs. (3.27) and (3.29) equated to zero may be solved simultaneously to obtain the relation

$$\eta \simeq \frac{1}{16}\left[1+x\frac{g'(x)}{g(x)}\right] \qquad \text{at critical.} \tag{3.30}$$

In the limit where the ions are point charges ($\gamma \to \infty$) we have $x = \varkappa/\gamma \to 0$. Taking into account the expressions for $g(x)$ [Eq. (3.28)] and of $g'(x) = -(1+x^2)^{-1}$, we observe that Eq. (3.30) locates the critical point at $\eta = 1/16$ for a binary electrolyte solution comprising spherical ions with embedded point charges. Or, in terms of the reduced total ionic density, $\rho\sigma^3 \simeq 0.12$.

Long needles ($\gamma \to 0$), on the other hand, correspond to the opposite limit $x \to \infty$. The behavior of $g(x)$ and $g'(x)$ at large x is

$$\begin{aligned} g(x) &= \frac{1}{x}\left[1 - \frac{1}{3}\frac{1}{x^2} + O\left(\frac{1}{x^4}\right)\right] \\ g'(x) &= -\frac{1}{x^2}\left[1 - \frac{1}{x^2} + O\left(\frac{1}{x^4}\right)\right], \end{aligned} \tag{3.31}$$

which, when inserted in Eq. (3.30) yields, to lowest order in $(1/x)$,

$$\eta = \frac{1}{24x^2} = \frac{\gamma^2}{24\varkappa^2} \qquad \text{at critical.} \tag{3.32}$$

At the same time, from the relation obtained by equating the right hand side of Eq. (3.27) to zero, we find

$$\varkappa^2 = \frac{8\pi^2\rho}{\varkappa g(x)} = \frac{48\pi\eta}{\gamma\sigma^3} \qquad \text{at critical,} \tag{3.33}$$

which can be used to substitute $\varkappa^2$ in Eq. (3.32) ($\gamma \to 0$) to obtain

$$\eta = \frac{1}{24}\sqrt{\frac{\gamma^3\sigma^3}{2\pi}} \qquad \text{at critical.} \tag{3.34}$$

This result shows how the critical density ρ_{crit} goes towards zero as $\gamma \to 0$ for elongated needles.

We can obtain an estimate for the critical temperature for needles ($\gamma \to 0$) from Eq. (3.33). Recalling the definition of $\varkappa^2$, Eq. (2.4), we have

$$\frac{\beta q^2}{\epsilon\sigma} = \frac{2\pi}{\gamma\sigma} \qquad \text{at critical.} \tag{3.35}$$

This relation indicates that T_{crit} is proportional to the inverse charge range parameter γ, and thus also goes to zero as $\gamma \to 0$.

4. POLYELECTROLYTE NEEDLES

4.1. Equation of State for Solutions of Polyelectrolytes

A polyelectrolyte solution consists of charged polymers and counterions that are point-like in comparison. As in Section 3, we will assume for simplicity that the polymers can be represented by straight needles aligned along the z-axis, while the much smaller counterions may be represented by point charges. By adopting this simple model of a polyelectrolyte solution, the results of Section 3 can be generalized in a straightforward way.

Let ρ_n and q_n be, respectively, the number density and the absolute value of the charge of the needles. Similarly, let ρ_c and q_c be the corresponding quantities for the counterions. Charge neutrality of the solution requires that

$$q_n\rho_n = q_c\rho_c. \tag{4.1}$$

For long polyelectrolytes the inequalities $q_n \gg q_c$ and $\rho_n \ll \rho_c$ apply. Furthermore, the Debye inverse-shielding length $\varkappa$ defined by Eq. (2.4) can be decomposed as

$$\varkappa^2 = \varkappa_n^2 + \varkappa_c^2, \tag{4.2}$$

where $\varkappa_i^2 = 4\pi\beta q_i^2\rho_i/\epsilon$ and $i = n, c$. The inequalities remarked above then imply that $\varkappa_n^2 \gg \varkappa_c^2$, so that to a first approximation $\varkappa^2 \simeq \varkappa_n^2$ holds.

Equations (3.1) and (3.2) describe the Coulomb interaction between any pair i and j of ions. If ion i is a polymer ion then the Fourier transform of its associated density is $\tilde{\Lambda}(\mathbf{k}) = \tilde{\lambda}(k_z)$; here for simplicity we adopt Eq. (3.12) for the charge density function. If, on the other hand, ion i is one of the counterions, then its associated charge density is simply $\tilde{\Lambda}(\mathbf{k}) = 1$. It follows that Eq. (3.10) is still applicable for the model polyelectrolyte solution, except that now the wavevector-dependent function $\varkappa^2(z)$ takes the slightly more complicated form

$$\varkappa^2(k_z) = \begin{cases} \varkappa_n^2 + \varkappa_c^2 \simeq \varkappa_n^2 & \text{for} \quad |k_z| < \gamma \\ \varkappa_c^2 & \text{for} \quad |k_z| > \gamma. \end{cases} \tag{4.3}$$

A consequence of the differences between Eqs. (3.14) and (4.3) is that I_q and P_q for the polyelectrolyte solution differ from the corresponding I_q, Eq. (3.15), and P_q, Eq. (3.21), for a solution of charged aligned needles. In particular, we not only have the previous k_z-integral in the range $|k_z| < \gamma$, but also we must account for the contributions from the k_z-integrals in the ranges $|k_z| > \gamma$, where $\varkappa^2(k_z)$ has the constant value $\varkappa_c^2$. This effect changes

Eq. (3.21) for the electrostatic contribution P_q to the osmotic pressure of the solution into

$$\beta P_q = -\frac{1}{24\pi^2}\{(\varkappa_n^2+\varkappa_c^2)^{3/2} f(x)+\varkappa_c^3[f(0)-f(\varkappa_c/\gamma)]\}, \tag{4.4}$$

in which $f(x)$ is the same auxilliary function introduced in Eq. (3.22). Notice, however, the new interpretation $x=\varkappa_n/\gamma$ of the variable x, which differs from the interpretation $x=\varkappa/\gamma$ in Sections 3.1 and 3.2. The special value of $f(x)$ at $x=0$ required in Eq. (4.4) is $f(0)=\pi$.

At the same time, the presence of counterions also modifies the equation of state of the reference (uncharged) system. To obtain the reference P_r, we must extend Eq. (3.23) to mixtures. The corresponding extension for mixtures was first reported by Lebowitz,[15] who used the Wertheim[16] Laplace-transform method to solve the Percus–Yevick integral equation for a mixture of hard spheres. Baxter[17] rederived and generalized the results of the mixture by using his Fourier transform factorization technique. The equation of state for a mixture of hard spheres is

$$\beta P_r = \rho\left[\frac{1}{1-\xi_3}+\frac{3\xi_1\xi_2}{\xi_0(1-\xi_3)^2}+\frac{3\xi_2^3}{\xi_0(1-\xi_3)^3}\right] \tag{4.5}$$

where

$$\xi_p = \frac{\pi}{6}\sum_i \rho_i\sigma_i^p, \qquad p=0,1,2,3, \tag{4.6}$$

with ρ_i the number density and σ_i the hard core diameter of species i. In our polyelectrolyte solution model the needles are considered to be equivalent to spheres of diameter σ_n, as pointed out following Eq. (3.23). The counterions, on the other hand, are represented by point charges of zero diameter (i.e., $\sigma_c=0$). Explicit evaluation of the ξ_p with Eq. (4.6) and subsequent substitution of the results into Eq. (4.5) yields, after some algebra

$$\beta P_r = \rho_n\left[\frac{1}{Q^2(1-\eta)}+\frac{1+\eta+\eta^2}{(1-\eta)^3}\right], \tag{4.7}$$

where the packing fraction $\eta=(\pi/6)\,\rho_n\sigma_n^3$ depends only on the number density ρ_n of the polyelectrolyte species. The parameter $Q\equiv\sqrt{q_c/q_n}=\sqrt{\rho_n/\rho_c}$ is a convenient measure of the charge asymmetry of the model.

Recognizing that $\rho_n/Q^2=\rho_c$, we see that P_r given by Eq. (4.7) is the pressure of a one-component system of hard spheres plus the ideal gas

pressure from the point particles in the available free volume between the hard spheres.

The osmotic pressure P (ideal plus excess contributions) of the polyelectrolyte solution is $P = P_r + P_q$, with P_q and P_r given, respectively, by Eqs. (4.4) and (4.7).

4.2. Critical Parameters for Solutions of Polyelectrolytes

As it was the case of solutions of charged aligned needles, we also find a region of the $T-\rho_n$ plane for which the inequality (3.24) is realized. In this region the model polyelectrolyte solution is unstable against phase separation into two liquid phases of different density of the binary polyelectrolyte. Following a similar approach to that of Section 3.3, we derive here simple analytical expressions for the parametric dependence of T_{crit} and $(\rho_n)_{\text{crit}}$ with the inverse charge range parameter γ and with the charge asymmetry parameter Q.

We begin by simplifying Eqs. (4.4) and (4.7). Equation (4.4) suggests that when $\varkappa_n^2 \gg \varkappa_c^2$ (or, equivalently, $Q^2 \ll 1$), the $\varkappa_c^3$-terms can be neglected:

$$\beta P_q \simeq -\frac{\varkappa_n^3}{24\pi^2} f(x). \tag{4.8}$$

This estimate has the same form as Eq. (3.21) for βP_q of a solution of charged aligned needles; closer examination reveals differences: $\varkappa_n$ replaces $\varkappa$ of Eq. (3.21) and x is now interpreted as $\varkappa_n/\gamma$.

It should be noticed that approximation (4.8) fails for very long needles. When $x \to \infty$ (which occurs when $\gamma \to 0$) the auxilliary function $f(x)$ behaves as

$$f(x) = \frac{3}{x} + \left(-\frac{2}{3} + 2\ln\frac{1}{x}\right)\frac{1}{x^3} + O\left(\frac{1}{x^5}\right). \tag{4.9}$$

It then follows from Eq. (3.21) that for

$$\gamma \leqslant \frac{f(0)}{3}\varkappa_c(\varkappa_c/\varkappa_n)^2 = (\pi/3)\, Q^2\, \varkappa_c \tag{4.10}$$

the term $\varkappa_c^3 f(0)$ becomes dominant and, consequently, Eq. (4.8) is inappropriate in this circumstance. With this caveat made clear, in the remaining of this section we approximate βP_q with Eq. (4.8) in order to derive approximate analytical expressions for the critical parameters of the solution.

With respect to Eq. (4.7) for βP_r, we assume: (i) that $\rho_c \gg \rho_n$, and (ii) that at the critical point $\eta = (\pi/6)\,\rho_n \sigma_n^3$ is very small. The first assumption applies to polyelectrolyte solutions with large charge asymmetry (small Q). The second assumption is similar to the simplification invoked in Section 3.3 for the analysis of the critical parameters in solutions of charged aligned needles; here it allows us to neglect the second term in Eq. (4.7). Further expansion of $(1-\eta)^{-1}$ in the first term finally gives

$$\beta P_r = \rho_c(1+\eta+\cdots). \tag{4.11}$$

The sum of Eqs. (4.8) and (4.11) gives us an approximate equation for βP that we can use to estimate the critical parameters of the solution. Differentiating once the approximate βP with respect to ρ_n and equating to zero (critical point) we find

$$\frac{1}{Q^2}(1+2\eta) - \frac{\varkappa_n^3}{8\pi^2\rho_n}\,g(x) = 0, \qquad \text{at critical.} \tag{4.12}$$

Differentiating this expression with respect to ρ_n and equating to zero gives

$$\frac{2\eta}{Q^2\rho_n} - \frac{\varkappa_n^3}{16\pi^2\rho_n^2}\,[g(x)+xg'(x)] = 0, \qquad \text{at critical.} \tag{4.13}$$

Solving Eqs. (4.12) and (4.13) for η gives [compare with Eq. (3.30)]

$$\eta = \frac{1}{4}\left[1 + x\frac{g'(x)}{g(x)}\right], \qquad \text{at critical.} \tag{4.14}$$

Taking now into account Eqs. (3.31) we reduce this expression to

$$\eta = \frac{\gamma^2}{6\varkappa_n^2}, \qquad \text{at critical.} \tag{4.15}$$

Solving Eq. (4.12) at large x [with the help of Eqs. (3.31)] gives the result

$$\varkappa_n^2 = \frac{48\pi\eta}{Q^2\gamma\sigma_n^3}, \qquad \text{at critical,} \tag{4.16}$$

which, when substituted on the right hand side of Eq. (4.15) produces

$$\eta = \frac{Q}{12}\sqrt{\frac{\gamma^3\sigma_n^3}{2\pi}}, \qquad \text{at critical.} \tag{4.17}$$

This result indicates that at critical the polyelectrolyte density $(\rho_n)_{\text{crit}}$ is proportional to the product $Q\gamma^{3/2}$. Thus, the dependence of $(\rho_n)_{\text{crit}}$ with the inverse charge range γ is similar to the dependence of ρ_{crit} with γ for solutions of charged aligned needles. For the polyelectrolyte case, however, $(\rho_n)_{\text{crit}}$ is also sensitive to the degree of charge asymmetry Q of the model: the larger the asymmetry (smaller Q) the smaller is $(\rho_n)_{\text{crit}}$.

We can now use Eq. (4.16) to estimate the critical temperature; we obtain

$$\frac{\beta q_n^2}{\epsilon\sigma_n} = \frac{2\pi}{Q^2\gamma\sigma_n}, \qquad \text{at critical.} \tag{4.18}$$

This result reveals that T_{crit} is proportional to $Q^2\gamma$. The dependence of T_{crit} with γ is the same as for solutions of charged aligned needles. Like $(\rho_n)_{\text{crit}}$, T_{crit} for the polyelectrolyte solution is also sensitive to degree of charge asymmetry Q of the model.

5. COEXISTENCE LINE AND CRITICAL PARAMETERS

In this section we present the results of numerical calculations for the dependence of the coexistence line with γ for solutions of charged aligned needles. We also investigate, for both the needle and the polyelectrolyte systems, the parametric dependence of the critical temperature and density with γ (solutions of needles) and with γ and Q (solutions of polyelectrolytes).

5.1. Charged Aligned Needles

It is convenient to express the thermodynamic properties of the solution in terms of reduced variables:

$$\text{(a)}\ \rho^* \equiv \rho\sigma^3; \qquad \text{(b)}\ \ T^* \equiv \epsilon k_{\text{B}} T\sigma/q^2; \qquad \text{(c)}\ \ P^* \equiv P\sigma^4\epsilon/q^2, \tag{5.1}$$

where σ is the diameter of a sphere with the same volume as the needles. An additional parameter, the reduced inverse charge range of a needle

$$\gamma^* \equiv \gamma\sigma, \tag{5.2}$$

is needed to complete the characterization of the state and features of a solution of needles. In terms of these variables the equation for the βP isotherm is [corresponds to the sum of Eqs. (3.21) and (3.23)]

$$\frac{P^*}{T^*} = \rho^* \frac{1+\eta+\eta^2}{(1-\eta)^3} - \frac{(\varkappa^*)^3}{24\pi^2} f(x), \tag{5.3}$$

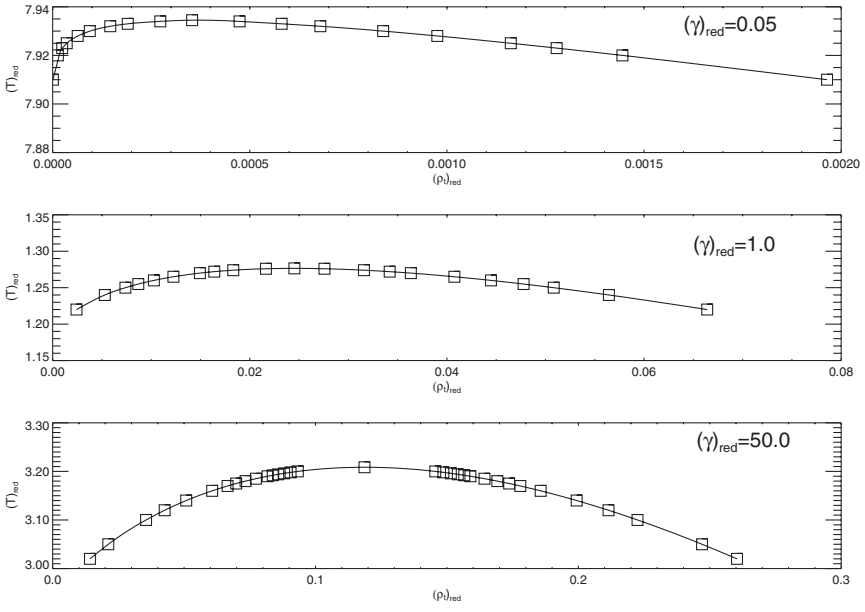

Fig. 1. Coexistence lines T^* versus ρ^* for solutions of needles with different reduced inverse charge range parameter. Top: $\gamma^* = 0.05$; Middle: $\gamma^* = 1.0$; Bottom: $\gamma^* = 50.0$. For convenience the y-scale of the graphs has been multiplied by the factor 1.0×10^3 (top) and 10.0 (middle and bottom).

where $\eta = (\pi/6)\,\rho^*$ and $\varkappa^* = \varkappa\sigma = \sqrt{4\pi\rho^*/T^*}$. The auxilliary function $f(x)$ was defined in Eq. (3.22), with $x = \varkappa/\gamma = \varkappa^*/\gamma^*$.

To determine the coexistence line, i.e., the densities $(\rho^*)'$ and $(\rho^*)''$ of the phases that coexist in equilibrium at temperature T^*, we implement the Maxwell equal area contruction for the P^*/T^* isotherm, Eq. (5.3).

In Fig. 1 we report the coexistence lines T^* versus ρ^* for solutions of needles characterized by three values of the reduced charge size parameter: $\gamma^* = 50.0$, $\gamma^* = 1.0$, and $\gamma^* = 0.05$. The figure shows that as γ^* decreases (i.e., the needles are longer), both critical parameters T^*_{crit} and ρ^*_{crit} decrease. It is also revealed that the degree of asymmetry of the coexistence line (as measured by the absolute value of the slopes of the low and high density branches) increases as γ^* decreases.

In Fig. 2 we represent the parametric dependence of T^*_{crit} and ρ^*_{crit} with the inverse range charge parameter γ^*. The critical parameters displayed are those associated with γ^* in the range $0.05 \leqslant \gamma^* \leqslant 10^5$. The upper right corner of the figure corresponds to very large values of γ^*, representative of binary electrolyte solutions with ions close to spherical in shape and with charge distribution of close to zero spatial extent. Conversely, the lower left

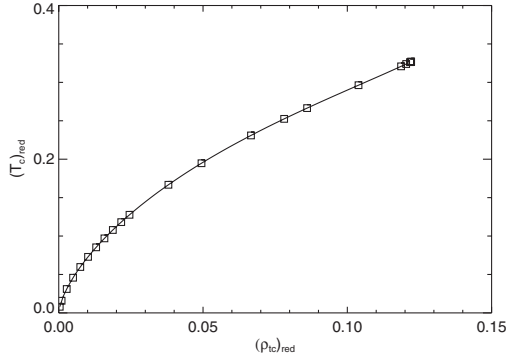

Fig. 2. Dependence of the critical parameters of solutions of needles with the reduced inverse charge range parameter γ^*. In every case $\partial(T^*)_{crit}/\partial\gamma^* > 0$ and $\partial(\rho_t^*)_{crit}/\partial\gamma^* > 0$. The behavior of the curve in the lower left corner agrees well with the estimates in Eq. (5.5).

corner of the figure corresponds to small values of γ^*; i.e., solutions comprising very long needles. The monotonous character of the curve is a reflection of the fact that $(\partial T^*_{crit}/\partial\gamma^*) > 0$ and $(\partial\rho^*_{crit}/\partial\gamma^*) > 0$ for every value of γ^*.

The analytical estimates for T^*_{crit} and ρ^*_{crit} derived in Section 3.3 apply to the behavior of the curve in the lower left corner of Fig. 2. In terms of reduced units formulas (3.34) and (3.35) are

$$\rho^*_{crit} = \frac{1}{2}\left(\frac{\gamma^*}{2\pi}\right)^{3/2}, \qquad T^*_{crit} = \frac{\gamma^*}{2\pi}, \tag{5.4}$$

which implies the relation (valid for very long needles)

$$T^*_{crit} = (\rho^*_{crit})^{2/3}. \tag{5.5}$$

5.2. Polyelectrolytes

To describe the model polyelectrolyte system we introduce the reduced variables

$$\text{(a)}\quad \rho_n^* \equiv \rho_n\sigma_n^3; \qquad \text{(b)}\quad T^* \equiv \epsilon k_B T\sigma_n/q_n^2; \qquad \text{(c)}\quad P^* \equiv P\sigma_n^4\epsilon/q_n^2, \tag{5.6}$$

where σ_n is the diameter of a sphere with the same volume as a polyelectrolyte needle. The two additional parameters that characterize the polyelectrolyte model are

$$\text{(d)}\quad \gamma^* \equiv \gamma\sigma_n \qquad \text{and} \qquad \text{(e)}\quad Q \equiv \sqrt{(q_c/q_n)}. \tag{5.7}$$

The equation for the osmotic pressure isotherm βP of our model polyelectrolyte solutions is given by the sum of Eqs. (4.4) and (4.7). In reduced units

$$\frac{P^*}{T^*} = \frac{P_r^*}{T^*} + \frac{P_q^*}{T^*}, \tag{5.8}$$

where

$$\frac{P_r^*}{T^*} = \rho_n^* \left[\frac{1}{Q^2(1-\eta)} + \frac{1+\eta+\eta^2}{(1-\eta)^3} \right], \tag{5.9}$$

$$\frac{P_q^*}{T^*} = -\frac{(\varkappa_n^*)^3}{24\pi^2} \{(1+Q^2)^{3/2} f(x) + Q^3 [\pi - f(Qx)]\}, \tag{5.10}$$

where $\eta = (\pi/6)\, \rho_n^*$, $\varkappa_n^* = \varkappa_n \sigma_n$, and $x = \varkappa_n/\gamma = \varkappa_n^*/\gamma^*$.

The shape of the coexistence line for our model polyelectrolyte solutions, and its dependence with γ^*, are qualitatively very similar to the curves reported in Fig. 1 for solutions of charged aligned needles. Here we focus on the dependence of the critical parameters T_{crit}^* and $(\rho_n^*)_{\text{crit}}$ with the model parameters γ^* and Q.

In Fig. 3 we represent the parametric dependence of T_{crit}^* and $(\rho_n^*)_{\text{crit}}$ with the inverse range charge parameter γ^* for two values, $Q = 0.005$ and $Q = 0.02$, of the charge asymmetry parameter of the model. The critical parameters displayed span the interval $0.05 \leqslant \gamma^* \leqslant 10^6$. As in Fig. 2, the upper right part of the curve corresponds to very large values of γ^*, representative of solutions in which the polyelectrolyte ionic species is close to spherical in shape, and has a charge distribution with close to zero spatial

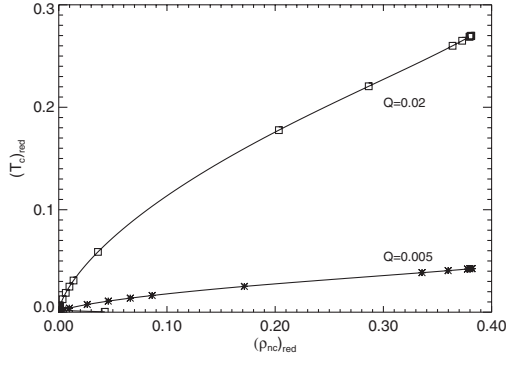

Fig. 3. Dependence of the critical parameters of polyelectrolyte solutions with the reduced inverse charge range parameter γ^* for two values of the charge asymmetry parameter Q. For convenience the y-scale has been multiplied by 100.0. In every case $(\partial T_{\text{crit}}^*/\partial\gamma^*) > 0$. However, for γ^* sufficiently low $(\partial(\rho_n^*)_{\text{crit}}/\partial\gamma^*) < 0$, as illustrated in Fig. 4 in detail.

extent. Conversely, the lower left part of the curves corresponds to small values of γ^*; i.e., solutions in which the polyelectrolyte species is a very long needle. At first sight the curves in this figure closely resemble the curve if Fig. 2 for charged aligned needles. Notice, however, the difference between the scales of the x- and y-axis of both figures.

In terms of reduced units, Eqs. (4.17) and (4.18) are

$$\rho^*_{\text{crit}} = Q\left(\frac{\gamma^*}{2\pi}\right)^{3/2}, \qquad T^*_{\text{crit}} = Q^2\left(\frac{\gamma^*}{2\pi}\right), \tag{5.11}$$

which implies the relation (valid for long needles; see below, however)

$$T^*_{\text{crit}} = Q^{4/3}(\rho^*_{\text{crit}})^{2/3}. \tag{5.12}$$

This relation is well satisfied in the lower left corner of the figure. But a more careful examination of the figure reveals that, for very small values of γ^* (long polyelectrolyte needles) $(\partial(\rho^*_n)_{\text{crit}}/\partial\gamma^*)$ becomes negative. This is illustrated in more detail in Fig. 4.

The effect may be explained by the fact that at very small γ^* Eq. (4.8) [that was used to derive the estimates (5.11) for the critical parameters] is qualitatively incorrect; in the regime indicated by Eq. (4.10), $\gamma^* < (\pi/3)\, Q^3 \varkappa^*_n$, the term $Q^3[\pi - f(Qx)]$ dominantes in Eq. (5.10).

6. SUMMARY

We have implemented a very simple extension of the Debye–Hückel approximation to study the thermodynamic properties and the phase

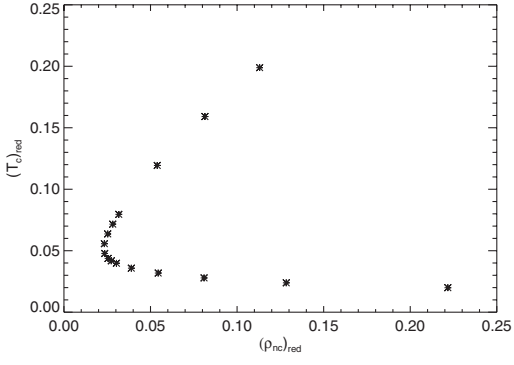

Fig. 4. Dependence of the critical parameters of polyelectrolyte solutions with γ^* in the case $Q = 0.005$. For convenience the x- and y-scales have been multiplied by, respectively, 1.0×10^3 and 1.0×10^5. In contrast to solutions of charged aligned needles, for polyelectrolyte solutions with γ^* sufficiently low $(\partial(\rho^*_n)_{\text{crit}}/\partial\gamma^*) < 0$.

diagram of ionic solutions comprising ions with a *charge distribution of a sizeable spatial extent* (in contrast to the embedded single point charge models, for which the charge distribution has zero spatial extent). The models considered here may be viewed, conceptually, as generated by deforming the spherical ions of the common models into ellipsoids that are strictly aligned in the z-direction (while keeping the volume of the ion constant); at the same time the original ionic point-charge distribution $q\,\delta(\mathbf{r})$ is deformed to $q\,\Lambda(\mathbf{r})$, where the charge distribution function $\Lambda(\mathbf{r})$ is spread only along the direction of the deformation. The "spatial extent" of $\Lambda(\mathbf{r})$ is characterized by an *inverse range* parameter γ, such that $\gamma \to \infty$ corresponds to an ion with an embedded point charge. For sufficiently long deformations, corresponding to the limit $\gamma \to 0$, the ions resemble rigid parallel needles. It should be noticed that our treatment does not impose any constraint on the ions in the transversal (i.e., x and y) directions.

We examined in detail the sensitivity of the coexistence line and the location of the critical point with the inverse range parameter γ for two solution models:

(a) Solutions comprising both cationic and anionic needles that are identical in every respect except for the charge sign.

(b) Solutions in which only one of the ionic species is made up of parallel rigid needles, while the other species is made up of point ions.

Clearly, system (a) is the analog, for ionic needles, of the familiar restricted primitive model of electrolytes, while system (b) is a very simple model for a polyelectrolyte solution.

For both systems we found that the critical density ρ_{crit} goes to zero as the length of the needles is increased to large values (the limit $\gamma \to 0$). For the polyelectrolyte model, however, for γ smaller than than a treshold value [corresponding to the onset of inequality (4.10)], the critical density of the solution actually increases with further elongation of the polyion species.

For the polyelectrolyte system, our results also shed light on the marked sensitivity of the coexistence line and of the critical parameters with the degree of charge asymmetry $Q = \sqrt{q_c/q_n}$ between a polyion and the counterion.

APPENDIX A: CORRELATION FUNCTIONS FOR NEEDLES

A straightforward way of obtaining the ion–ion correlation functions $h_{ij}(\mathbf{r})$ within the Debye–Hückel approximation is to solve the Ornstein–Zernike integral equations

$$\tilde{\mathsf{h}}(\mathbf{k}) = \tilde{\mathsf{c}}(\mathbf{k}) + \tilde{\mathsf{c}}(\mathbf{k})\,\rho\,\tilde{\mathsf{h}}(\mathbf{k}), \tag{A.1}$$

where $\tilde{\mathsf{h}}(\mathbf{k})$ and $\tilde{\mathsf{c}}(\mathbf{k})$ are 2×2 square matrices with elements $\tilde{h}_{ij}(\mathbf{k})$ and $\tilde{c}_{ij}(\mathbf{k})$, respectively the three dimensional Fourier transforms of the ion–ion correlation functions $h_{ij}(\mathbf{r})$ and $c_{ij}(\mathbf{r})$. Equation (A.1) is formally solved for $\tilde{\mathsf{h}}(\mathbf{k})$ as

$$\tilde{\mathsf{h}}(\mathbf{k}) = (\mathbf{1} - \rho\tilde{\mathsf{c}}(\mathbf{k}))^{-1}\,\tilde{\mathsf{c}}(\mathbf{k}), \tag{A.2}$$

where $\mathbf{1}$ is the unit matrix. Within the Debye–Hückel approximation, the matrix of direct correlation functions takes the dyadic form

$$\tilde{\mathsf{c}}(\mathbf{k}) = -\beta\tilde{\psi}(\mathbf{k}) = -\frac{4\pi\beta F(k_z)}{\epsilon k^2}\,|\mathbf{q})(\mathbf{q}|, \tag{A.3}$$

where $|\mathbf{q})$ is the column vector with elements q and $-q$, and $(\mathbf{q}|$ is the corresponding transpose row vector. The second equality follows directly from Eqs. (2.2) and (3.2)–(3.6).

With Eq. (A.3) the right hand side of Eq. (A.2) may be easily calculated with the help of the Sherman–Morrison formula;[18] we find that the ij element of $\tilde{\mathsf{h}}(\mathbf{k})$ has the expression

$$\tilde{h}_{ij}(\mathbf{k}) = -\frac{(4\pi\beta/\epsilon)\,F(k_z)\,q_i q_j}{k^2 + \varkappa^2(k_z)}, \tag{A.4}$$

with $\varkappa^2(k_z)$ given by Eq. (3.7). To obtain the $\mathbf{r}$-space form of the correlation function we must perform the inverse Fourier transform

$$h_{ij}(\mathbf{r}_\perp, z) = -\frac{4\pi\beta q_i q_j}{\epsilon}\int_{-\infty}^{\infty}\frac{dk_z}{2\pi}\,\mathrm{e}^{-ik_z z}\,F(k_z)\int\frac{d^2\mathbf{k}_\perp}{(2\pi)^2}\,\frac{\mathrm{e}^{-i\mathbf{k}_\perp\cdot\mathbf{r}_\perp}}{k_z^2 + k_\perp^2 + \varkappa^2(k_z)}, \tag{A.5}$$

in which $\mathbf{r}_\perp$ and $\mathbf{k}_\perp$ are, respectively, the two dimensional vectors (x, y) and (k_x, k_y). In polar coordinates $d^2\mathbf{k}_\perp = d\phi\, dk_\perp k_\perp$; the integration with respect to ϕ is immediate:[19]

$$h_{ij}(\mathbf{r}_\perp, z) = -\frac{4\pi\beta q_i q_j}{\epsilon}\int_{-\infty}^{\infty}\frac{dk_z}{2\pi}\,\mathrm{e}^{-ik_z z}\,F(k_z)\int_0^{\infty}\frac{dk_\perp}{(2\pi)}\,\frac{k_\perp J_0(k_\perp r_\perp)}{k_z^2 + k_\perp^2 + \varkappa^2(k_z)}, \tag{A.6}$$

where J_0 is the Bessel function of order zero. The inner integral can be performed in closed form;[20] one obtains (taking into account the even character of the argument of the inner integral with respect to k_z)

$$h_{ij}(r_\perp, z) = -\frac{2\beta q_i q_j}{\pi\epsilon} \int_0^\infty dk_z \cos(k_z z)\, F(k_z)\, K_0(\sqrt{\varkappa^2(k_z)+k_z^2}\, r_\perp), \tag{A.7}$$

where K_0 is the modified Bessel function of order zero.[19, 20]

To proceed further, we must specify the functions $F(k_z)$ and $\varkappa^2(k_z)$. Here we adopt the expression, Eq. (3.14), that corresponds to the simple model (3.12) for the Fourier transform $\tilde{\lambda}(k_z)$ of the charge density of a needle. Considering specifically the transverse correlations between needles whose centers lie at the same height (that is $z = 0$), Eq. (A.7) reduces to

$$h_{ij}(r_\perp, 0) = -\frac{2\beta q_i q_j}{\pi\epsilon} \int_0^\gamma dk_z\, K_0(\sqrt{\varkappa^2+k_z^2}\, r_\perp). \tag{A.8}$$

When needles are very long, $\gamma \simeq 0$, the integral may be approximated as

$$h_{ij}(r_\perp, 0) = -\frac{2\gamma\beta q_i q_j}{\pi\epsilon} K_0(\varkappa r_\perp). \tag{A.9}$$

The modified Bessel function has the asymptotic behavior[19, 20]

$$K_0(\varkappa r_\perp) = \left(\frac{\pi}{2}\right)^{1/2} \frac{e^{-\varkappa r_\perp}}{(\varkappa r_\perp)^{1/2}} \left[1 - \frac{1}{8\varkappa r_\perp} + O((\varkappa r_\perp)^{-3/2})\right], \tag{A.10}$$

from which we conclude that for long needles $h_{ij}(r_\perp, 0)$ behaves at large $r_\perp$ according to

$$h_{ij}(r_\perp, 0) = -\left(\frac{2}{\pi}\right)^{1/2} \frac{\gamma\beta q_i q_j}{\epsilon} \frac{e^{-\varkappa r_\perp}}{(\varkappa r_\perp)^{1/2}}. \tag{A.11}$$

ACKNOWLEDGMENTS

We dedicate this work to Michael Fisher on the occasion of his 70th anniversary. F.O.R., G.S., and J.R. gratefully acknowledge the support of the Division of Chemical Sciences, Office of Basic Energy Sciences, Office of Energy Research, U.S. Department of Energy.

REFERENCES

1. M. E. Fisher, *J. Stat. Phys.* **75**:1 (1994).
2. G. Stell, *J. Stat. Phys.* **78**:197 (1995).
3. W. G. McMillan and J. E. Mayer, *J. Chem. Phys.* **13**:276 (1945).
4. H. L. Friedman, *A Course in Statistical Mechanics* (Prentice–Hall, Englewood Cliffs, New Jersey, 1985).
5. F. O. Raineri, J. Routh, and G. Stell, *J. Phys. IV France* **10**:(Pr5-95) (2000).
6. J. M. Romero-Enrique, G. Orkoulas, A. Z. Panagiotopoulos, and M. E. Fisher, *Phys. Rev. Lett.* **85**:4558 (2000).
7. Q. L. Yan and J. J. de Pablo, *Phys. Rev. Lett.* **86**:2054 (2001).
8. A. Z. Panagiotopoulos and M. E. Fisher, *Phys. Rev. Lett.* **88**:045701 (2002).
9. H. Xu, H. L. Friedman, and F. O. Raineri, *J. Solution Chem.* **20**:739 (1991).
10. T. L. Hill, *An Introduction to Statistical Thermodynamics* (Addison–Wesley, Reading, Mass., 1960).
11. Y. Levin, X.-J. Li, and M. E. Fisher, *Phys. Rev. Lett* **73**:2716 (1994).
12. See, e. g. G. A. Corri and M. Muthukumar, *J. Chem. Phys.* **111**:1765 (1999).
13. J.-P. Hansen and I. R. McDonald, *Theory of Simple Liquids*, 2nd. edn. (Academic Press, London, 1990).
14. J. L. Lebowitz and J. W. Perram, *Mol. Phys.* **50**:1207 (1983).
15. J. L. Lebowitz, *Phys. Rev. A* **133**:895 (1964).
16. M. S. Wertheim, *Phys. Rev. Lett.* **10**:321 (1963).
17. R. F. Baxter, *J. Chem. Phys.* **52**:4559 (1970).
18. T. Kailath, *Linear Systems* (Prentice–Hall, Englewood Cliffs, New Jersey, 1980).
19. M. Abramowitz and I. A. Stegun, *Handbook of Mathematical Functions* (Dover Publications, New York, 1972).
20. N. N. Lebedev, *Special Functions and their Application* (Dover Publications, New York, 1972).